

## Response to Reviewer #1

There are several minor or major concerns for this paper.

1. Only observed precipitation, air temperature and precipitation deficit/surplus were shown in the Figure 1. How reliable are the simulations with and without the dynamic vegetation (DV)? Also, what's the performance of the simulated historical Leaf area index (LAI) by the DV version?

>> We understand it is critical to evaluate the model performance but this study builds upon previous studies (Wang et al., 2016; Yu et al., 2016; Erfanian et al., 2016) that documented model performances with and without the vegetation dynamics. As per the reviewer's comments, we clarified these points as follows:

Line 91: *“Wang et al. (2016) extensively evaluated the RegCM-CLM-CN-DV model for simulating regional climate and ecosystems in West Africa. It was performed using the lateral boundary conditions (LBCs) from the ERA-Interim, and with and without vegetation dynamics. Yu et al. (2016) and Erfanian et al. (2016) also examined the impacts of vegetation dynamics on the climate and ecosystems with multiple LBCs from past and future GCM simulations. Building upon these previous studies, this study investigates the impacts of vegetation dynamics on the regional drought characteristics, i.e., frequency, duration, and severity over the focal regions of the West African domain: the Sahel, the Gulf of Guinea, and the Congo Basin (Fig. 1).”*

Line 118: *“This study briefly presents the present-day climate, vegetation, and droughts simulated with RegCM-CLM-CN-DV with and without vegetation dynamics, based on detailed evaluations of model performance in previous studies with the same model, i.e., Wang et al. (2016), Yu et al. (2016) and Erfanian et al. (2016).”*

Regarding the performance of LAI, Fig. 3c presents the LAI difference between DV and SV. We have revised the paragraph to clarify this as follows:

Line 152: *“With the addition of vegetation dynamics, the LAI is overestimated in the Guinea Gulf and the central Congo Basin, and it is underestimated in the Sahel region and southern and northern parts of the Congo Basin, whereas in the case without vegetation dynamics, the LAI represents Moderate Resolution Imaging Spectroradiometer-based monthly-varying climatological values (Figs. 3a, 3b, and 3e). Over the Sahel, the model underestimates the woody plants and grasses with significant overestimation of the bare ground area, which can be attributed to biases in the CLM-CN-DV as well as the RCM physical climate, i.e., dry bias (Wang et al., 2016; Erfanian et al., 2016).”*

2. LAI has been used as one of the main indicators representing the responses of land surface to regional climate change. For the DV version, what will the plant functional types (PFTs) change with different climate scenarios? How may the regional climate changes be associated with the projected land surface changes including vegetation (e.g., PFTs area extent and tree height) induced changes in energy and water fluxes?

>> As per the reviewer's suggestion, we have revised the manuscript to relate changes of LAI with changes of vegetation types as well as the surface conditions that follow. However, note that those have been well documented in our previous studies (Wang et al., 2016; Yu et al., 2016; Erfanian et al., 2016; refer to Fig. R1), so we have added the explanations without additional figures to keep our focus on drought characteristics.

Line 210: *“As examined in Erfanian et al. (2016), along with lower LAI in the Sahel, with DV in comparison to SV, higher albedo, lower cooling, lower evapotranspiration, and lower precipitation is simulated as strong land-atmosphere coupling is known in the region like Sahel. Also note that such changes in LAI do not always accompany changes in the dominant vegetation types. In the Sahel, there will be more grass in future with increased LAI, and changes in land cover from grasses to woody plants are found in the Gulf of Guinea.”*

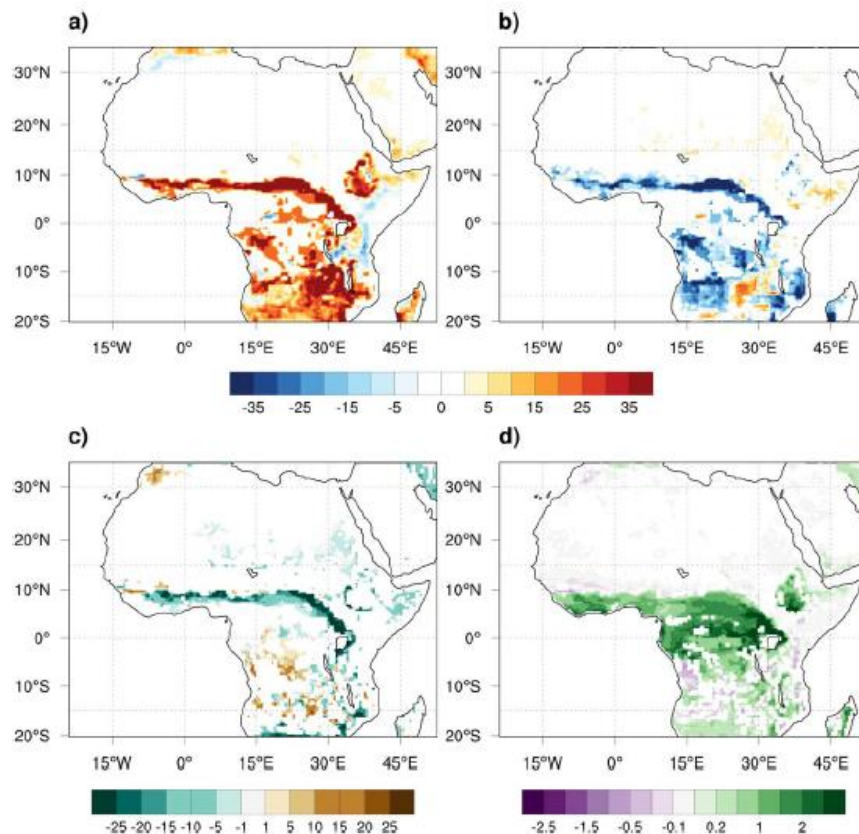


**Figure 7.** Future changes of annual fractional coverage (%) of (a) woody plants, (b) grasses, (c) bare ground, and (d) future changes of annual LAI for MME of RCM-CLM-CNDV simulations as of 2081–2100 compared with 1981–2000. Shading is applied only to areas where changes pass the 1% significance test.

*Fig. R1. Changes of vegetation fractions in the future (Erfanian et al., 2016)*

3. Were any differences between the DV and SV or between the future and historical periods statistically different?

>> As per reviewer's comments, we have added dots to the difference figures (Fig. 2, 3, 4, 5 and 7) to identify the statistically significant differences, with an example of Fig. 3 below.

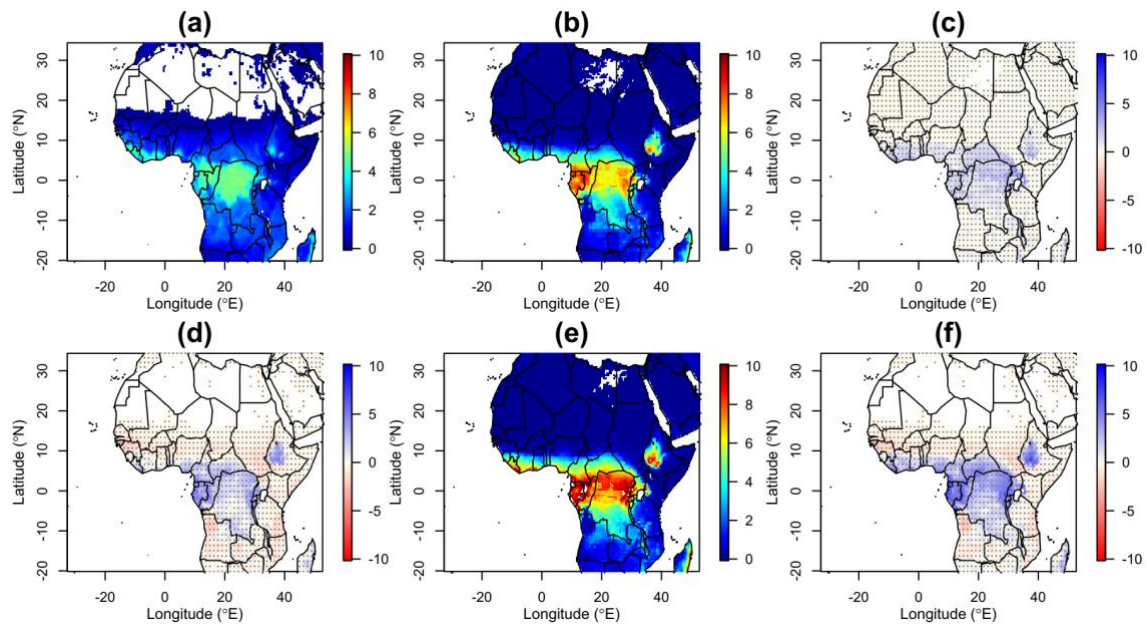


Figure 3. Averages of leaf area index (LAI) (a) used for SV and (b) simulated in DV ensembles for the historical period (1981–2000), and (c) their differences (DV-SV). And, we show (d) the difference between future (2081–2100) and historical periods in DV, (e) averages of simulated LAI in DV ensembles for future period, and (f) the difference between DV and SV in the future period. Doted regions show areas passing the two-tailed confidence level with  $\alpha=0.01$ .

4. There is no any discussion in this paper. It's needed because people got to know why and how your present work is important and unique, and what the limitations and next steps are.

>> We have expanded the Conclusions and Discussion sections with discussion about the importance and limits of this study as well as future study directions.

Line 251: “While most future drought characterization studies with climate model predictions have been carried out without considering the role of vegetation (e.g., Cook et al., 2015; Huang et al, 2018), this study suggests the necessity of the comprehensive understanding of biosphere–atmosphere interactions in future drought projections. Furthermore, it has been pointed out that such land–atmosphere feedbacks could exacerbate droughts under future climate projections (Dirmeyer et al., 2013; Zhou et al., 2019). Therefore, these drought studies could be critical over not only the Sahel but also over other regions where positive feedbacks between land and atmosphere are strong, such as the interior of North America (Kim and Wang, 2007; Wang et al., 2007).

The present study uses the SPEI via calculating PET with the Thornthwaite approach, which considers air temperature as a governing feature of PET. However, there are various other methods to calculate PET, and among them, the Penman–Montieth method could be another candidate that could be employed for the SPEI because it includes many other variables (i.e., humidity, radiation coefficient, and wind speed) to calculate PET. Other climatic conditions affecting PET may balance temperature rise (McVicar et al., 2012), and thus, further investigations with multiple

*approaches could shed a light on future drought characteristics.*

*This study points out the potentially prolonged and enhanced drought events over the Sahel. In addition, many African countries are expected to experience population growth, and a majority of the population increase rate is found in Niger and Chad, which are neighboring countries in the Sahel (Ahmadalipur et al., 2019). Combined with the high likelihood of prolonged and enhanced drought, population growth and, thus, the associated increase in water demand will likely exacerbate the risks of future drought and will present challenges for climate change adaptation for managing water needs in the region.”*

# Projected effects of vegetation feedback on drought characteristics of West Africa using a coupled regional land–vegetation–climate model

<sup>1</sup>Muhammad Shafqat Mehboob, <sup>1</sup>Yeonjoo Kim, <sup>1</sup>Jaehyeong Lee, <sup>2</sup>Myoung-Jin Um, <sup>3</sup>Amir Erfanian, <sup>4</sup>Guiling Wang

<sup>1</sup>Department of Civil and Environmental Engineering, Yonsei University, Seoul, 03722, South Korea  
<sup>2</sup>Department of Civil Engineering, Kyonggi University, Suwon-si Gyeonggi-do, 16227, South Korea  
<sup>3</sup>Department of Atmospheric and Oceanic Sciences, University of California, Los Angeles, 90095, USA  
<sup>4</sup>Department of Civil and Environmental Engineering, University of Connecticut, Storrs, 06269, USA

**Correspondence:** Yeonjoo Kim (yeonjoo.kim@yonsei.ac.kr)

**Abstract.** This study investigates the projected effect of vegetation feedback on drought conditions in West Africa using a regional climate model coupled to the National Center for Atmospheric Research Community Land Model, the carbon-nitrogen (CN) module, and the dynamic vegetation (DV) module (RegCM-CLM-CN-DV). The role of vegetation feedback is examined based on simulations with and without the DV module. Simulations from four different global climate models are used as lateral boundary conditions (LBCs) for historical and future periods (i.e., historical: 1981–2000; future: 2081–2100). With utilizing the Standardized Precipitation Evapotranspiration Index (SPEI), we quantify the frequency, duration and severity of droughts over the focal regions of the Sahel, the Gulf of Guinea, and the Congo Basin. With the vegetation dynamics being considered, future droughts become more prolonged and enhanced over the Sahel, whereas for the Guinea Gulf and Congo Basin, the trend is opposite. Additionally, we show that simulated annual leaf greenness (i.e., the Leaf Area Index) well-correlates with annual minimum SPEI, particularly over the Sahel, which is a transition zone, where the feedback between land-atmosphere is relatively strong. Furthermore, we note that our findings based on the ensemble mean are varying, but consistent among three different LBCs except for one LBC. Our results signify the importance of vegetation dynamics in predicting future droughts in West Africa, where the biosphere and atmosphere interactions play a significant role in the regional climate setup.

## 1 Introduction

West Africa is significantly vulnerable to climate change yet, projecting its future climate is a challenging task (Cook, 2008). From the 1970s, a long period of drought was observed over West Africa, lasting until the late 1990s. While it is important to reduce the uncertainties and improve the reliability of future climate projections, there is still no clear consensus about whether the future outlook of the West African hydroclimate will be drier or wetter. Some studies projected drying trends (Hulme et al., 2001), whereas others predicted a wetter future (Hoerling et al., 2006; Kamga et al., 2005; Maynard et al., 2002). Caminade and Terray (2010) reviewed the A1B scenarios of the 21 coupled models from the Coupled Model Intercomparison Project

31 (CMIP) Phase 3 (CMIP3), which focused on a balanced emphasis on all energy resources, for the Sahel and found no clear  
32 evidence of precipitation trending over Africa. Roehrig et al. (2013) combined the CMIP3 and CMIP Phase 5 (CMIP5) global  
33 climate models (GCM) and found that western end of Sahel shows a drying trend whereas eastern Sahel shows opposite trend.  
34 Limited-area models, i.e., Regional Climate Models (RCMs) are often used as they can capture finer details as compared to  
35 GCMs (Kumar et al., 2008). The physics of RCMs dominate the signals imposed by large-scale forcing (i.e., forces with  
36 boundary conditions derived from GCMs). However, discrepancies still remain, because RCMs have distinct systematic errors  
37 with West African precipitation, varying in amplitude and pattern across models (Druyan et al., 2009; Paeth et al., 2011).

38 Because climate and greenhouse gas concentrations continuously change, a noticeable change in vegetation is  
39 expected (Yu et al., 2014b). A more representative and reliable model requires incorporation of dynamic vegetation (DV)  
40 instead of static vegetation (SV) (Alo and Wang, 2010; Patricola and Cook, 2010; Wramneby et al., 2010; Xue et al., 2012;  
41 Zhang et al., 2014). Charney et al. (1975) first conceptualized the idea that precipitation could change dynamically in response  
42 to vegetation variability, he claimed that changes in precipitation over the Sahel is due to reduction in vegetation and increase  
43 in albedo. Various studies of biosphere–atmosphere interactions have been documented (Wang and Eltahir, 2000; Patricola  
44 and Cook, 2008; Kim and Wang, 2007) but there are a few studies in which a coupled RCM-DV is used. Such studies are in  
45 their initial stages (Cook and Vizy, 2008; Garnaud et al., 2015; Wang et al., 2016; Yu et al., 2016). For example, Cook and  
46 Vizy (2008) introduced a coupled potential vegetation model into an RCM to estimate the influence of global warming on  
47 South American climate and vegetation. They found a reduction in vegetation cover of almost 70% in the Amazon rainforest  
48 highlighting the importance of using DV in RCMs. Recently, Wang et al. (2016) introduced a DV feature into the International  
49 Center for Theoretical Physics Regional Climate Model (RegCM4.3.4) (Giorgi et al., 2012) with Carbon–Nitrogen (CN)  
50 dynamics and DV (RegCM-CLM-CN-DV) of the community land model (CLM4.5) (Lawrence et al., 2011; Oleson et al.,  
51 2010). They validated the coupled model over tropical Africa (Wang et al., 2016; Yu et al., 2016). The advantage of simulating  
52 DV in the model eliminates potential discrepancies between the climate conditions and bioclimatic conditions required to  
53 prescribed vegetation, but it can create climate draft, i.e., biases in the model (Erfanian et al., 2016). Additionally, such a model  
54 is advantageous, because it provides a capacity to simulate future terrestrial ecosystems as the climate evolves.

55 Among various drought indices (e.g., the Palmer Draught Severity index (Palmer, 1965) and the Standard  
56 Precipitation Index (McKee et al., 1993)) used to assess drought events, Vicente–Serrano (2010) suggested the Standardized  
57 Precipitation Evapotranspiration Index (SPEI), which uses the deficit between precipitation and potential evapotranspiration.  
58 Since the development of SPEI, various researchers have adopted this index for drought studies (Boroneant et al., 2011; Deng,  
59 2011; Li et al., 2012a; Li et al., 2012b; Lorenzo–Lacruz et al., 2010; Paulo et al., 2012; Sohn et al., 2013; Spinoni et al., 2013;  
60 Wang et al., 2016; Yu et al., 2014a; Yu et al., 2014b). Abiodun et al. (2013) studied the climate change and corresponding  
61 extreme events caused by afforestation in Nigeria while defining the drought events using SPEI. McEvoy et al. (2012) used  
62 SPEI as a drought index to monitor conditions over Nevada and Eastern California, proposing that SPEI was a convenient tool  
63 to describe the drought in arid regions.

Deleted: et al.,

65 In this study, we aim to understand the impact of vegetation feedback on the future of droughts over West Africa.  
66 Specifically, SPEI is used to depict vegetation feedback on drought characteristics according to frequencies, severity, and  
67 duration over West Africa. Four sets of GCMs are used to force the RCM with and without vegetation dynamics. By comparing  
68 the drought characteristics between the two simulation sets, we show the signals of DV on the drought processes in different  
69 regions of Africa.

70 **2 Methodology**

71 **2.1 Model Description**

72 This study uses state-of-the-art RegCM-CLM-CN-DV (Wang et al., 2016). Specifically, RegCM4.3.4 (Giorgi et al., 2012) and  
73 CLM4.5 (Lawrence et al., 2011; Oleson et al., 2010) with CN dynamics and DV are coupled to simulate various atmospheric,  
74 land, biogeochemical, vegetation phenology, and vegetation distribution processes. RegCM is a regional model that uses an  
75 Arakawa B-grid finite differencing algorithm along with a terrain-following  $\sigma$ -pressure vertical coordinate system. Grell et al.  
76 (1994) introduced an additional dynamic component in the model that is taken from the hydrostatic version of the Pennsylvania  
77 State University Mesoscale Model version 5. From Community Climate Model (Kiehl et al., 1996) a radiation scheme was  
78 added. Model covers four different convection parameterization schemes namely 1) the modified-Kuo scheme (Anthes et al.,  
79 1987), 2) the Tiedtke scheme (Tiedtke, 1989), 3) the Grell scheme (Grell, 1993) and 4) the Emanuel scheme (Emanuel, 1991)  
80 along with non-local boundary layer scheme of Holtslag et al. (1990). Cloud and precipitation scheme comes from the physics  
81 package (Pal et al., 2000). Aerosols algorithm follows Solmon et al. (2006) and Zakey et al. (2006).

82 While solving a surface biogeochemical, biogeophysical, ecosystem dynamical and hydrological processes, CLM4.5  
83 considers fifteen soil layers, sixteen distinct plant functional types (PTF), up to five snow layers and a ordered data structure  
84 in each grid cell (Erfanian et al., 2016; Lawrence et al., 2011; Wang et al., 2016). An optional component present in this model  
85 is the CN and DV module. CN module not only simulates CN cycles and plant phenology and maturity but also estimates  
86 vegetation height, stem area index and leaf area index (LAI). The DV module projects the fractional coverage of different  
87 PFTs and corresponding temporary variations at yearly time steps developed using CN-estimated carbon budget, also it  
88 accounts for plant existence, activity and formation. If CN and DV modules are inactive, it means that the distribution and  
89 vegetation composition in the model is established according to observed data sets (i.e., SV).

90 **2.2 Numerical Experiments**

91 Wang et al. (2016) extensively evaluated the RegCM-CLM-CN-DV model for simulating regional climate and ecosystems in  
92 West Africa. It was performed using the lateral boundary conditions (LBCs) from the ERA-Interim, and with and without  
93 vegetation dynamics. Yu et al. (2016) and Erfanian et al. (2016) also examined the impacts of vegetation dynamics on the  
94 climate and ecosystems with multiple LBCs from past and future GCM simulations. Building upon these previous studies, this

Moved (insertion) [1]

Moved (insertion) [2]

Deleted: This study focuses



study investigates the impacts of vegetation dynamics on the regional drought characteristics, i.e., frequency, duration, and severity over the focal regions of the West African domain; the Sahel, the Gulf of Guinea, and the Congo Basin (Fig. 1). As presented in Erfanian et al. (2016), a total of 16 different numerical simulations are performed (Table 1). Numerical simulation is carried out in two distinct configurations, one in which CN-DV module is activated (i.e. DV runs) and the other in which CN-DV module is not activated (i.e., SV runs). Additionally, the LBCs for the RCMs are derived from four GCMs: the Community Earth System Model (Kay et al., 2015), the Geophysical Fluid Dynamics Laboratory model, the Model for Interdisciplinary Research on the Climate–Earth System Model (Watanabe et al., 2011), and the Max Planck Institute Earth System Model. These eight simulations are performed for two different periods: the present (i.e., 1981–2000) (CMIP5-historical) and the future (i.e., 2081–2100) (CMIP5-RCP8.5). The model grid is configured using a 50-km horizontal grid spacing and 18 vertical layers from the surface to 50 hPa. The model parameterizations are the same as the one used by previous studies of Wang et al. (2016), Yu et al. (2016) and Erfanian et al. (2016).

**Deleted:** region with emphasis on three regions over the study  
**Deleted:** (see Fig. 1):  
**Deleted:** . A  
**Deleted:** To investigate the impacts of DV,  
**Deleted:** of model

**Deleted:** .

**Moved up [1]:** Yu et al.  
**Deleted:** (2016), which was optimized with previous applications over the same region (Alo and Wang, 2010; Saini et al., 2015; Wang and Alo, 2012; Yu et al., 2014b). Its performance and simulation details with ERA-interim and future projections were documented by  
**Moved down [3]:** Wang et al.  
**Moved up [2]:** (2016) and Erfanian et al.  
**Deleted:** Wang et al. (2016) and  
**Deleted:** (2016), respectively.

## 2.3 SPEI

Vicente-Serrano et al. (2010) gave a simple approach to estimate SPEI. Thornthwaite (1948) method is used to calculate monthly PET in first step, this method utilizes three parameters 1) temperature, 2) latitude and 3) time. For a given month,  $j$ , and year,  $i$ , the monthly water surplus or deficit, ( $D_{i,j}$ ) is calculated by Eq. (1) given below.

$$D_{i,j} = PR_{i,j} - PET_{i,j} \quad (1)$$

Where PR is precipitation and PET is potential evapotranspiration. In the second step accumulated monthly water deficits, ( $X_{i,j}^k$ ), at time scale  $k$  (i.e., 12 months) in a given month,  $j$ , and year,  $i$ , is calculated based on  $D$ . Finally,  $SPEI_{i,j}^k$  is estimated by fitting  $X_{i,j}^k$  to the log-logistic distribution by mean of the L-moments method by (Hosking 1990). In this study, we define a drought event with an  $SPEI_{i,j}^k$  of less than -1.

## 3 Results Analysis

**Deleted:** and Discussions

### 3.1 Historical Climate, Vegetation and Drought

This study briefly presents the present-day climate, vegetation, and droughts simulated with RegCM-CLM-CN-DV with and without vegetation dynamics, based on detailed evaluations of model performance in previous studies with the same model, i.e., Wang et al. (2016), Yu et al. (2016) and Erfanian et al. (2016). Relative to the observational data from the University of Delaware (Fig. 1), both SV and DV ensembles (Figs. 2a and 2b) follow the observed spatial patterns of precipitation and air temperature with overestimating precipitation over Gulf of Guinea and the northern and southern parts of the Congo Basin. But over Sahel and the central Congo Basin it is underestimated. The spatial trend of temperature bias is almost similar to precipitation bias, with the dry and warm bias occur simultaneously and vice versa. It also reflects how evaporative cooling plays an important role in surface energy flux across the regions (Erfanian et al., 2016). Additionally, the model generally performs better with SV than with DV. The biases of precipitation and temperature in SV ensembles are further amplified in

**Deleted:** ,  
**Deleted:** as  
**Deleted:** , including  
**Moved (insertion) [3]**  
**Deleted:** performance according to different RCMs, which was already provided by



49 the DV ensembles. DV tends to remove the physical inconsistencies linked with SV, but it increases the sensitivity of the  
50 model to lateral boundary conditions (LBC) and potential model biases related to LBCs (Erfanian et al., 2016). So, we can say  
51 that one of the benefits to introduce DV in the model is that it gives us a clear signal that how the change of vegetation could  
52 impact climate forcings, presented in Sections 3.2 and 3.3.

53 ~~With the addition of~~ vegetation dynamics, the LAI is overestimated in the Guinea Gulf and the central Congo Basin,  
54 and it is underestimated in the Sahel region and southern and northern parts of the Congo Basin, ~~whereas in~~ the case without  
55 vegetation dynamics, where the LAI represents Moderate Resolution Imaging Spectroradiometer-based monthly-varying  
56 climatological values (Figs. 3a, 3b, and 3c). ~~Over the Sahel, the model underestimates the woody plants and grasses with~~  
57 ~~significant overestimation of the bare ground area, which can be attributed to biases in the CLM-CN-DV as well as the RegCM~~  
58 ~~physical climate, i.e., dry bias (Wang et al., 2016; Erfanian et al., 2016).~~ Such dry biases lead to warm bias in air temperate  
59 via the reduction of evaporative cooling.

60 The precipitation surplus/deficit (Eq. (1), Fig. 2c) was used in calculating SPEI values to analyze the drought  
61 frequency. Precipitation minus potential evapotranspiration is mainly controlled by air temperature according to Thornthwaite  
62 method. The difference of DV and SV ensembles for the precipitation surplus/deficit (Fig. 2c-3) follow that of the precipitation  
63 and temperature, as expected. ~~Therefore, the difference for the drought frequency (Fig. 4a) depicts a similar pattern.~~ For  
64 historical period over Sahel drought frequency is up to 44% higher when DV is enabled whereas it is 40% less over the Gulf  
65 of Guinea. Such characteristics in the ensemble averages are captured in the difference of drought frequency between DV and  
66 SV of each ensemble member to different extents (the first row of Fig. 5). While the Sahel and the Guinea Coast regions  
67 present relatively similar differences in the drought frequency, the central Congo Basin shows quite different trends among  
68 the different LBCs. CCSM presents increase in drought frequency in DV relative to SV, but MIROC presents the opposite.  
69 GFDL and MPI-ESM presents relatively weak differences.

70 To investigate the role of vegetation dynamics on drought severity and duration, the averages of SPEI over three  
71 regions are estimated in Fig. 6. In the Sahel, the more severe and longer droughts are clearly captured for the present-day DV  
72 ensemble compared to the SV ensemble. As noted, the reason behind an underestimated LAI over Sahel is dry biasness in  
73 atmospheric forcings, which then leads to an additional decrease in precipitation in that region. Thus, prolonged and severe  
74 drought events are consistently found in DV ensembles for Sahel. In the Guinea Coast and the Congo, the opposite is found  
75 because of the vegetation dynamics. Also, different LBCs present consistent patterns except for CCSM, which shows limited  
76 differences of SPEI between DV and SV in the regional averages over the Congo and Gulf of Guinea.

### 77 3.2 Predicted Future Climate, Vegetation, and Droughts

78 In this section, we focus on the projected future climate, vegetation, and droughts, simulated with and without vegetation  
79 dynamics. First of all, projected precipitation in the future period of both SV and DV ensembles (Figs. 7a and 7b) shows the  
80 similar spatial patterns to that of the past with different regional changes. In the SV ensemble (Fig. 7a-3), small decrease in  
81 precipitation are found in Sahel and the Congo Basin. For the DV ensemble (Fig. 7a-4), it is clearly visible that the band of

Deleted: By allowing

Deleted: compared to

Deleted: 3a, 3b, and 3c). It seems that underestimated LAI over the Sahel region is due to dry bias in the atmospheric forcings, which then leads to additional decreases in precipitation for that region.

Deleted: .

89 precipitation below 10 °N increases up to 56.4 m/month. As expected, atmospheric warming caused by the increased CO<sub>2</sub>  
90 concentration in the future scenario leads to widespread increases in temperatures for both SV and DV ensembles (Figs. 7b-3  
91 and 7b-4).

92 Consistent with such changes in climate conditions, ~~changes in LAI~~ because of atmospheric warming and CO<sub>2</sub>  
93 fertilization. In the DV ensemble (Figs. 3d and 3e), widespread increases in future LAI are found, compared to that from the  
94 historical period over the regions below 10 °N. Beyond 10 °N, vegetation cover is sparse and there are no noticeable changes  
95 in future LAI. Note that LAI does not differ for both historical or future periods in SV.

96 In the future, the precipitation surplus/deficit shows a general decline for both SV and DV ensembles (Figs. 7c-3 and  
97 7c-4). Only local increases in precipitation surplus/deficit near 10 °N are captured by the DV ensemble. Such changes in  
98 precipitation surplus/deficit lead to similar changes in drought frequencies between the future and historical periods for both  
99 SV and DV ensembles (Figs. 4b and 4c). Corresponding to the band of precipitation increase, a slight decrease of drought  
00 frequency of up to 15 % is shown in the DV ensemble.

### 01 3.3 Impact of ~~Vegetation Dynamics on Future Droughts~~

02 It is desired to include vegetation dynamic component in land-atmospheric coupled model for future climate projections,  
03 although including this property makes the model more complex but it is closer to a realistic model. In this section, we focus  
04 on the role of vegetation dynamics in future ensembles (i.e., the difference between DV and SV for the future).

05 Investigating the difference of LAI between DV and SV for the future period (Fig. 3f), we find that the LAI for the  
06 DV ensemble is smaller than that of SV over the Sahel and larger below 10 °N. ~~LAI differences between SV and DV ensembles,~~  
07 show quite similar patterns both in historical and future periods (Figs. 3c and 3f) with LAI biases caused by ~~the biases from~~  
08 ~~both CLM-CN-DV and RegCM~~ in the historical period being similarly shown in the future period. Note that underestimated  
09 LAI in Sahel is not necessarily a bias in the future simulations, because the future LAI in SV is assumed to be identical to  
10 historical climatological LAI as in historical SV ensemble.

11 Differences between DV and SV in precipitation and air temperature (Figs. ~~7a-5 and 7b-5~~) follow the LAI differences.  
12 ~~As examined in Erfanian et al. (2016), along with lower LAI in the Sahel, with DV in comparison to SV, higher albedo, lower~~  
13 ~~cooling, lower evapotranspiration, and lower precipitation is simulated as strong land-atmosphere coupling is known in the~~  
14 ~~region like Sahel. Also note that such changes in LAI do not always accompany changes in the dominant vegetation types. In~~  
15 ~~the Sahel, there will be more grass in future with increased LAI, and changes in land cover from grasses to woody plants are~~  
16 ~~found in the Gulf of Guinea.~~

17 Over the region below 10 °N, wetter and colder climate conditions are predicted with the DV ensemble compared to  
18 the SV ensemble, resulting in increased precipitation surplus, as shown in Fig. 7c-5. Consequently, the frequencies of drought  
19 events decrease up to 40 % over Gulf of Guinea and increases up to 43 % over the Sahel based on the ensemble averages (Fig.  
20 4d). Among the runs with different LBCs, the inconsistency in the drought frequency is found over the central Congo Basin  
21 with CCSM, as already pointed out in the historical simulations.

Deleted: vegetation state (i.e., LAI)

Formatted: Indent: First line: 0.5"

Deleted: vegetation dynamics on future droughts

Formatted: Indent: First line: 0.5"

Deleted: Such different responses of vegetation can be attributed to dominant vegetation types over the regions as grasses and trees are dominant over the Sahel and below the 10°N respectively. We note that

Deleted: climate

Deleted: 7a-5 and 7b-5) follow the differences of the vegetation state (i.e., LAI).

31 The differences of regional averages of SPEI over the three different regions (see the last rows in each panel of Fig.  
32 6) present the impact of vegetation dynamics on future drought severity and duration. Ensemble averages show that more  
33 prolonged and more severe droughts are projected over the Sahel and vice versa for the Guinea Gulf and the Congo Basin.  
34 Among ensemble members with different LBCs, CCSM presents a bit different results from other LBCs, not capturing the  
35 decreased droughts for the Guinea Gulf and the Congo Basin.

36 We next present the correlation coefficients between annual maximum LAI and annual minimum SPEI over the  
37 regions for both historical and future periods (Fig. 8). With drought events, as reflected in the relatively lower annual minimum  
38 SPEI, the annual maximum LAI should be smaller, because leaf growth is limited during such events. Such interactive  
39 responses of vegetation to climate conditions are only captured in the DV ensemble. When DV is active, a large portion of  
40 West Africa has a strong positive association between the maximum LAI and minimum SPEI. Relatively strong correlations  
41 are found along the Sahel, which may attribute to the fact that feedback between land–atmosphere is relatively strong in  
42 transition zones.

#### 43 4 Conclusion and Discussion

44 In this study, we employed the drought index (i.e., SPEI) to quantitatively assess the effects of vegetation dynamics on  
45 projected future drought over West Africa. The impact of vegetation feedback on drought projection was examined both with  
46 and without considering vegetation dynamics. This study suggests that, with the vegetation dynamics considered, drought is  
47 prolonged and enhanced over the Sahel, whereas for the Guinea Gulf and Congo Basin, the trend is clearly the opposite. Such  
48 opposite changes could attribute to amplified biases because a feedback exists between climate and vegetation in a dynamic  
49 vegetation model, as well as due to bioclimatic inconsistency in the static vegetation model. These results are quite consistent  
50 over 3 different LBCs while the LBC with CCSM show somewhat opposite results for the Congo Basin. Furthermore, we  
51 show that simulated annual leaf greenness (i.e., LAI) was well correlated with annual minimum SPEI, particularly over the  
52 Sahel, which is a sensitive, transition zone, where the feedback between land–atmosphere is relatively strong.

53 ~~While most future drought characterization studies with climate model predictions have been carried out without~~  
54 ~~considering the role of vegetation (e.g., Cook et al., 2015; Huang et al, 2018), this study suggests the necessity of the~~  
55 ~~comprehensive understanding of biosphere–atmosphere interactions in future drought projections. Furthermore, it has been~~  
56 ~~pointed out that such land–atmosphere feedbacks could exacerbate droughts under future climate projections (Dirmeyer et al.,~~  
57 ~~2013; Zhou et al., 2019). Therefore, these drought studies could be critical over not only the Sahel but also over other regions~~  
58 ~~where positive feedbacks between land and atmosphere are strong such as the interior of North America (Kim and Wang,~~  
59 ~~2007).~~

60 The present study uses the SPEI via calculating PET with the Thornthwaite approach, ~~which~~ considers air temperature  
61 as a governing feature of PET. ~~However, there are various other methods to calculate PET, and among them, the Penman–~~  
62 ~~Montieth method could be another candidate that could be employed for the SPEI because it includes~~ many other variables

Deleted: We note that the

Deleted: that

Deleted: There

Deleted: method one of

Deleted: is

Deleted: method that that include

69 (i.e., humidity, radiation coefficient, and wind speed) to calculate PET. Other climatic conditions affecting PET may balance  
70 temperature rise (McVicar et al., 2012), and thus, further investigations with multiple approaches could shed a light on future  
71 drought characteristics.

**Deleted:** Due to temperature rise, there may be limited effects on drought via increased PET because other

**Deleted:** for

**Deleted:** ).

72 This study points out the potentially prolonged and enhanced drought events over the Sahel. In addition, many African  
73 countries are expected to experience population growth, and a majority of the population increase rate is found in Niger and  
74 Chad, which are neighbouring countries in the Sahel (Ahmadalipour et al., 2019). Combined with the high likelihood of  
75 prolonged and enhanced drought, population growth and, thus, the associated increase in water demand will likely exacerbate  
76 the risks of future drought and will present challenges for climate change adaptation for managing water needs in the region.  
77 As examined in Erfanian et al. (2016), along with lower LAI in the Sahel, with DV in comparison to SV, higher albedo, lower  
78 cooling, lower evapotranspiration, and lower precipitation is simulated as strong land-atmosphere coupling is known in the  
79 region like Sahel. Also note that such changes in LAI do not always accompany changes in the dominant vegetation types. In  
80 the Sahel, there will be more grass in future with increased LAI, and changes in land cover from grasses to woody plants are  
81 found in the Gulf of Guinea.

82 *Data Availability.* Observed data was collected from University of Delaware and model output data are available in  
83 [https://github.com/yjkim1028/RegCM-CN-DV\\_data](https://github.com/yjkim1028/RegCM-CN-DV_data). In addition, a map with the country boundaries is drawn with 'mapdata'  
84 package of R-studio.

85 *Author contribution.* YK and GW designed the study and AE performed the simulations. MSM, JH and MU performed the  
86 results analysis. MSM, YK, AE and GW wrote the manuscript.

87 *Competing interests.* The authors declare that they have no conflict of interest.

88 *Acknowledgements.* This study was supported by the Basic Science Research Program through the National Research  
89 Foundation of Korea, which was funded by the Ministry of Science, ICT & Future Planning (2018R1A1A3A04079419) and  
90 the Internationalization Infra Fund of Yonsei University (2018 Fall semester).

## 91 References

- 92 Abiodun, B. J., Salami, A. T., Matthew, O. J., and Odedokun, S.: Potential impacts of afforestation on climate change and  
93 extreme events in Nigeria, *Climate dynamics*, 41, 277-293, 2013.
- 94 Ahmadalipour, A., Moradkhani, H., Castelletti, A., and Magliocca, N.: Future drought risk in Africa: Integrating  
95 vulnerability, climate change, and population growth, *Science of the Total Environment*, 662, 672-686, 2019.
- 96 Alo, C. A., and Wang, G.: Role of dynamic vegetation in regional climate predictions over western Africa, *Climate*  
97 *dynamics*, 35, 907-922, 2010.
- 98 Anthes, R. A., Hsie, E.-Y., and Kuo, Y.-H.: Description of the Penn State/NCAR mesoscale model version 4 (MM4), NCAR  
99 Boulder, CO., 1987.

04 Boroneant, C., Ionita, M., Brunet, M., and Rimbu, N.: CLIVAR-SPAIN contributions: seasonal drought variability over the  
05 Iberian Peninsula and its relationship to global sea surface temperature and large scale atmospheric circulation, WCRP  
06 OSC: Climate Research in Service to Society, 24-28, 2011.

07 Caminade, C., and Terray, L.: Twentieth century Sahel rainfall variability as simulated by the ARPEGE AGCM, and future  
08 changes, *Climate Dynamics*, 35, 75-94, 2010.

09 Charney, J., Stone, P. H., and Quirk, W. J.: Drought in the Sahara: a biogeophysical feedback mechanism, *science*, 187, 434-  
10 435, 1975.

11 Cook, K. H.: Climate science: the mysteries of Sahel droughts, *Nature Geoscience*, 1, 647, 2008.

12 Cook, K. H., and Vizy, E. K.: Effects of twenty-first-century climate change on the Amazon rain forest, *Journal of Climate*,  
13 21, 542-560, 2008.

14 Cook, K. H., Vizy, E. K., Launer, Z. S., and Patricola, C. M.: Springtime intensification of the Great Plains low-level jet and  
15 Midwest precipitation in GCM simulations of the twenty-first century, *Journal of Climate*, 21, 6321-6340, 2008.

16 [Cook, B. I., Ault, T. R., and Smerdon, J. E.: Unprecedented 21st century drought risk in the American Southwest and Central  
17 Plains, \*Science Advances\*, 1, e1400082, 2015.](#)

18 [Dirmeyer, P. A., Jin, Y., Singh, B., and Yan, X.: Trends in land-atmosphere interactions from CMIP5 simulations, \*Journal  
19 of Hydrometeorology\*, 14, 829-849, 2013.](#)

20 Deng, F.: Global CO<sub>2</sub> Flux Inferred From Atmospheric Observations and Its Response to Climate Variabilities, 2011.

21 Druryan, L. M., Fulakeza, M., Lonergan, P., and Noble, E.: Regional climate model simulation of the AMMA Special  
22 Observing Period# 3 and the pre-Helene easterly wave, *Meteorology and atmospheric physics*, 105, 191-210, 2009.

23 Emanuel, K. A.: A scheme for representing cumulus convection in large-scale models, *Journal of the Atmospheric Sciences*,  
24 48, 2313-2329, 1991.

25 Erfanian, A., Wang, G., Yu, M., and Anyah, R.: Multimodel ensemble simulations of present and future climates over West  
26 Africa: Impacts of vegetation dynamics, *Journal of Advances in Modeling Earth Systems*, 8, 1411-1431, 2016.

27 Garnaud, C., Sushama, L., and Versegny, D.: Impact of interactive vegetation phenology on the Canadian RCM simulated  
28 climate over North America, *Climate Dynamics*, 45, 1471-1492, 2015.

29 Giorgi, F., Coppola, E., Solmon, F., Mariotti, L., Sylla, M., Bi, X., Elguindi, N., Diro, G., Nair, V., and Giuliani, G.:  
30 RegCM4: model description and preliminary tests over multiple CORDEX domains, *Climate Research*, 52, 7-29, 2012.

31 Grell, G. A.: Prognostic evaluation of assumptions used by cumulus parameterizations, *Monthly Weather Review*, 121, 764-  
32 787, 1993.

33 Grell, G. A., Dudhia, J., and Stauffer, D. R.: A description of the fifth-generation Penn State/NCAR mesoscale model  
34 (MM5), 1994.

35 Hoerling, M., Hurrell, J., Eischeid, J., and Phillips, A.: Detection and attribution of twentieth-century northern and southern  
36 African rainfall change, *Journal of climate*, 19, 3989-4008, 2006.

37 Holtslag, A., De Bruijn, E., and Pan, H.: A high resolution air mass transformation model for short-range weather  
38 forecasting, *Monthly Weather Review*, 118, 1561-1575, 1990.

39 [Huang, J., Zhai, J., Jiang, T., Wang, Y., Li, X., Wang, R., Xiong, M., Su, B., and Fischer, T.: Analysis of future drought  
40 characteristics in China using the regional climate model CCLM, \*Climate dynamics\*, 50, 507-525, 2018.](#)

41 Hulme, M., Doherty, R., Ngara, T., New, M., and Lister, D.: African climate change: 1900-2100, *Climate research*, 17, 145-  
42 168, 2001.

43 Kamga, A. F., Jenkins, G. S., Gaye, A. T., Garba, A., Sarr, A., and Adedoyin, A.: Evaluating the National Center for  
44 Atmospheric Research climate system model over West Africa: Present- day and the 21st century A1 scenario, *Journal  
45 of Geophysical Research: Atmospheres*, 110, 2005.

46 Kay, J., Deser, C., Phillips, A., Mai, A., Hannay, C., Strand, G., Arblaster, J., Bates, S., Danabasoglu, G., and Edwards, J.:  
47 The Community Earth System Model (CESM) large ensemble project: A community resource for studying climate  
48 change in the presence of internal climate variability, *Bulletin of the American Meteorological Society*, 96, 1333-1349,  
49 2015.

50 Kiehl, T., Hack, J., Bonan, B., Boville, A., Briegleb, P., Williamson, L., and Rasch, J.: Description of the NCAR community  
51 climate model (CCM3), 1996.

52 [Kim, Y., and Wang, G.: Impact of vegetation feedback on the response of precipitation to antecedent soil moisture anomalies  
53 over North America, \*Journal of Hydrometeorology\*, 8, 534-550, 2007.](#)

54 Kumar, S. V., Peters-Lidard, C. D., Eastman, J. L., and Tao, W.-K.: An integrated high-resolution hydrometeorological  
55 modeling testbed using LIS and WRF, *Environmental Modelling & Software*, 23, 169-181, 2008.

56 Lawrence, D. M., Oleson, K. W., Flanner, M. G., Thornton, P. E., Swenson, S. C., Lawrence, P. J., Zeng, X., Yang, Z. L.,  
57 Levis, S., and Sakaguchi, K.: Parameterization improvements and functional and structural advances in version 4 of the  
58 Community Land Model, *Journal of Advances in Modeling Earth Systems*, 3, 2011.

59 Li, W.-G., Yi, X., Hou, M.-T., Chen, H.-L., and Chen, Z.-L.: Standardized precipitation evapotranspiration index shows  
60 drought trends in China, *Chinese Journal of Eco-Agriculture*, 20, 643-649, 2012a.

61 Li, W., Hou, M., Chen, H., and Chen, X.: Study on drought trend in south China based on standardized precipitation  
62 evapotranspiration index, *Journal of Natural Disasters*, 21, 84-90, 2012b.

63 Lorenzo-Lacruz, J., Vicente-Serrano, S. M., López-Moreno, J. I., Beguería, S., García-Ruiz, J. M., and Cuadrat, J. M.: The  
64 impact of droughts and water management on various hydrological systems in the headwaters of the Tagus River  
65 (central Spain), *Journal of Hydrology*, 386, 13-26, 2010.

66 Maynard, K., Royer, J.-F., and Chauvin, F.: Impact of greenhouse warming on the West African summer monsoon, *Climate  
67 Dynamics*, 19, 499-514, 2002.

68 McEvoy, D. J., Huntington, J. L., Abatzoglou, J. T., and Edwards, L. M.: An evaluation of multiscalar drought indices in  
69 Nevada and eastern California, *Earth Interactions*, 16, 1-18, 2012.

70 McKee, T. B., Doesken, N. J., and Kleist, J.: The relationship of drought frequency and duration to time scales, *Proceedings*  
71 *of the 8th Conference on Applied Climatology*, 1993, 179-183,

72 McVicar, T. R., Roderick, M. L., Donohue, R. J., Li, L. T., Van Niel, T. G., Thomas, A., Grieser, J., Jhajharia, D., Himri, Y.,  
73 and Mahowald, N. M.: Global review and synthesis of trends in observed terrestrial near-surface wind speeds:  
74 Implications for evaporation, *Journal of Hydrology*, 416, 182-205, 2012.

75 Oleson, K. W., Lawrence, D. M., Gordon, B., Flanner, M. G., Kluzek, E., Peter, J., Levis, S., Swenson, S. C., Thornton, E.,  
76 and Feddes, J.: Technical description of version 4.0 of the Community Land Model (CLM), 2010.

77 Paeth, H., Hall, N. M., Gaertner, M. A., Alonso, M. D., Moumouni, S., Polcher, J., Ruti, P. M., Fink, A. H., Gosset, M., and  
78 Lebel, T.: Progress in regional downscaling of West African precipitation, *Atmospheric science letters*, 12, 75-82, 2011.

79 Pal, J. S., Small, E. E., and Eltahir, E. A.: Simulation of regional- scale water and energy budgets: Representation of subgrid  
80 cloud and precipitation processes within RegCM, *Journal of Geophysical Research: Atmospheres*, 105, 29579-29594,  
81 2000.

82 Palmer, W. C.: Meteorological drought. Research Paper No. 45. Washington, DC: US Department of Commerce, Weather  
83 Bureau, 59, 1965.

84 Patricola, C., and Cook, K. H.: Atmosphere/vegetation feedbacks: A mechanism for abrupt climate change over northern  
85 Africa, *Journal of Geophysical Research: Atmospheres*, 113, 2008.

86 Patricola, C. M., and Cook, K. H.: Northern African climate at the end of the twenty-first century: an integrated application  
87 of regional and global climate models, *Climate Dynamics*, 35, 193-212, 2010.

88 Paulo, A., Rosa, R., and Pereira, L.: Climate trends and behaviour of drought indices based on precipitation and  
89 evapotranspiration in Portugal, *Natural Hazards and Earth System Sciences*, 12, 1481-1491, 2012.

90 Roehrig, R., Bouniol, D., Guichard, F., Hourdin, F., and Redelsperger, J.-L.: The present and future of the West African  
91 monsoon: A process-oriented assessment of CMIP5 simulations along the AMMA transect, *Journal of Climate*, 26,  
92 6471-6505, 2013.

93 Saini, R., Wang, G., Yu, M., and Kim, J.: Comparison of RCM and GCM projections of boreal summer precipitation over  
94 Africa, *Journal of Geophysical Research: Atmospheres*, 120, 3679-3699, 2015.

95 Sohn, S. J., Ahn, J. B., and Tam, C. Y.: Six month-lead downscaling prediction of winter to spring drought in South Korea  
96 based on a multimodel ensemble, *Geophysical Research Letters*, 40, 579-583, 2013.

97 Solmon, F., Giorgi, F., and Liousse, C.: Aerosol modelling for regional climate studies: application to anthropogenic  
98 particles and evaluation over a European/African domain, *Tellus B: Chemical and Physical Meteorology*, 58, 51-72,  
99 2006.

00 Spinoni, J., Antofie, T., Barbosa, P., Bihari, Z., Lakatos, M., Szalai, S., Szentimrey, T., and Vogt, J.: An overview of drought  
01 events in the Carpathian Region in 1961–2010, *Advances in Science and Research*, 10, 21-32, 2013.

02 Tiedtke, M.: A comprehensive mass flux scheme for cumulus parameterization in large-scale models, *Monthly Weather*  
03 *Review*, 117, 1779-1800, 1989.

**Deleted:** Spinoni, J., Naumann, G., Carrao, H., Barbosa, P., and  
Vogt, J.: World drought frequency, duration, and severity for  
1951–2010, *International Journal of Climatology*, 34, 2792-2804,  
2014. .



08 Vicente-Serrano, S. M., Beguería, S., and López-Moreno, J. I.: A multiscalar drought index sensitive to global warming: the  
 09 standardized precipitation evapotranspiration index, *Journal of climate*, 23, 1696-1718, 2010a.

10 Wang, G., and Eltahir, E. A.: Ecosystem dynamics and the Sahel drought, *Geophysical Research Letters*, 27, 795-798, 2000.

11 Wang, G., Yu, M., Pal, J. S., Mei, R., Bonan, G. B., Levis, S., and Thornton, P. E.: On the development of a coupled  
 12 regional climate-vegetation model RCM-CLM-CN-DV and its validation in Tropical Africa, *Climate dynamics*, 46,  
 13 515-539, 2016.

14 Watanabe, S., Hajima, T., Sudo, K., Nagashima, T., Takemura, T., Okajima, H., Nozawa, T., Kawase, H., Abe, M., and  
 15 Yokohata, T.: MIROC-ESM: model description and basic results of CMIP5-20c3m experiments, *Geoscientific Model*  
 16 *Development Discussions*, 4, 1063-1128, 2011.

17 Wramneby, A., Smith, B., and Samuelsson, P.: Hot spots of vegetation- climate feedbacks under future greenhouse forcing  
 18 in Europe, *Journal of Geophysical Research: Atmospheres*, 115, 2010.

19 Xue, Y., Boone, A., and Taylor, C. M.: Review of recent developments and the future prospective in West African  
 20 atmosphere/land interaction studies, *International Journal of Geophysics*, 2012, 2012.

21 Yu, M., Li, Q., Hayes, M. J., Svoboda, M. D., and Heim, R. R.: Are droughts becoming more frequent or severe in China  
 22 based on the standardized precipitation evapotranspiration index: 1951–2010?, *International Journal of Climatology*, 34,  
 23 545-558, 2014a.

24 Yu, M., Wang, G., Parr, D., and Ahmed, K. F.: Future changes of the terrestrial ecosystem based on a dynamic vegetation  
 25 model driven with RCP8. 5 climate projections from 19 GCMs, *Climatic change*, 127, 257-271, 2014b.

26 Yu, M., Wang, G., and Pal, J. S.: Effects of vegetation feedback on future climate change over West Africa, *Climate*  
 27 *dynamics*, 46, 3669-3688, 2016.

28 Zakey, A., Solmon, F., and Giorgi, F.: Implementation and testing of a desert dust module in a regional climate model,  
 29 *Atmospheric Chemistry and Physics*, 6, 4687-4704, 2006.

30 Zhang, W., Jansson, C., Miller, P. A., Smith, B., and Samuelsson, P.: Biogeophysical feedbacks enhance the Arctic  
 31 terrestrial carbon sink in regional Earth system dynamics, *Biogeosciences*, 11, 5503-5519, 2014.

32 Zhou, S., Williams, A. P., Berg, A. M., Cook, B. I., Zhang, Y., Hagemann, S., Lorenz, R., Seneviratne, S. I., and Gentile, P.:  
 33 Land-atmosphere feedbacks exacerbate concurrent soil drought and atmospheric aridity, *Proceedings of the National*  
 34 *Academy of Sciences*, 201904955, 2019.

**Deleted:** and Alo, C. A.: Changes in precipitation seasonality in West Africa predicted by RegCM3 and the impact of dynamic vegetation feedback, *International Journal of Geophysics*, 2012, 2012. ... [1]

**Formatted:** EndNote Bibliography, Indent: Left: 0", Hanging: 2 ch, First line: -2 ch, Space After: 0 pt, Line spacing: 1.5 lines

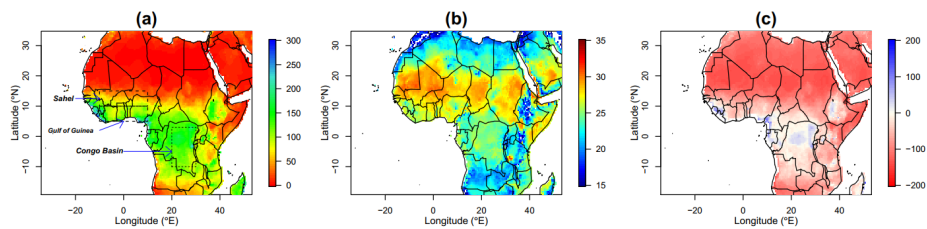


**Figure 1.** Observed averages of (a) precipitation (mm/month) and (b) air temperature (°C) from 1981–2000 using datasets from the University of Delaware, and (c) derived precipitation deficit/surplus (mm/month). In (a), the boxes with the dashed lines show three focal regions of Sahel, Gulf of Guinea and the Congo Basin.

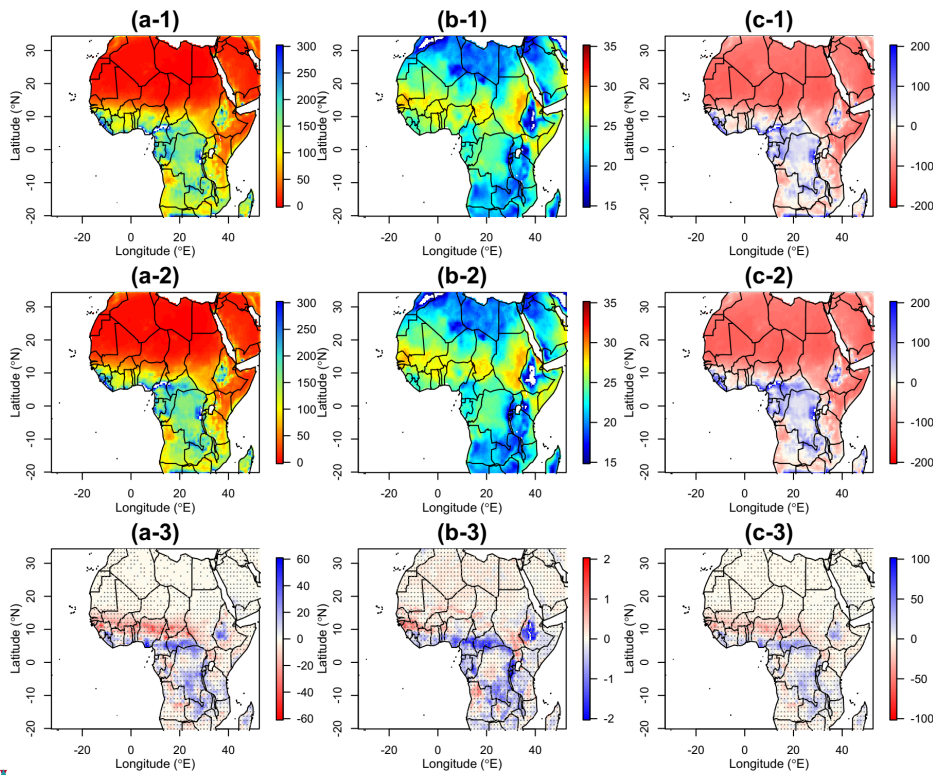


**Figure 2.** Averages of simulated (a) precipitation (mm/month), (b) temperature (°C), and (c) derived precipitation surplus/deficit (mm/month) from 1) SV ensembles, 2) DV ensembles, and 3) the difference between DV and SV ensembles for the historical period of 1981–2000. Dotted region shows areas passing the two-tailed confidence level with  $\alpha=0.01$ .

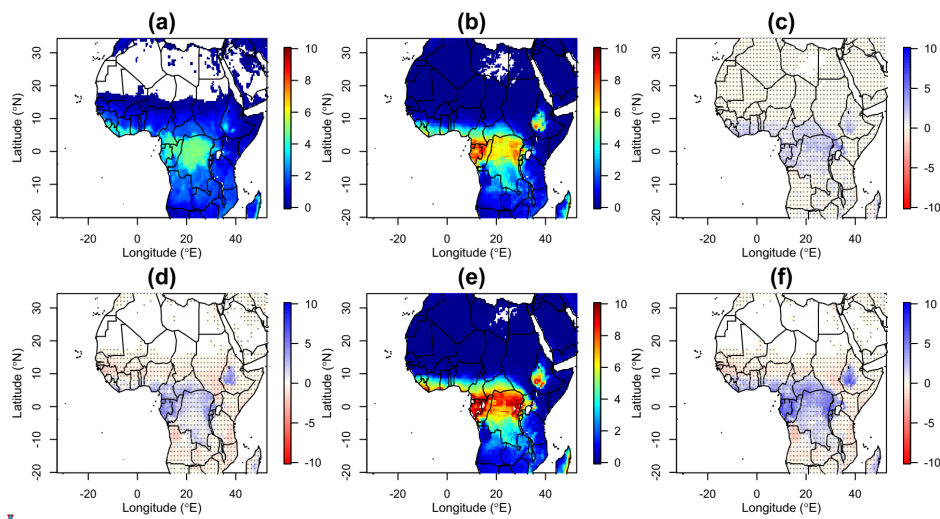


**Figure 3.** Averages of leaf area index (LAI) (a) used for SV and (b) simulated in DV ensembles for the historical period (1981–2000), and (c) their differences (DV-SV). And, we show (d) the difference between future (2081-2100) and historical periods in DV, (e) averages of simulated LAI in DV ensembles for future period, and (f) the difference between DV and SV in the future period. Dotted regions show areas passing the two-tailed confidence level with  $\alpha=0.01$ .

Deleted:

Formatted: Font color: Text 1

Deleted: )

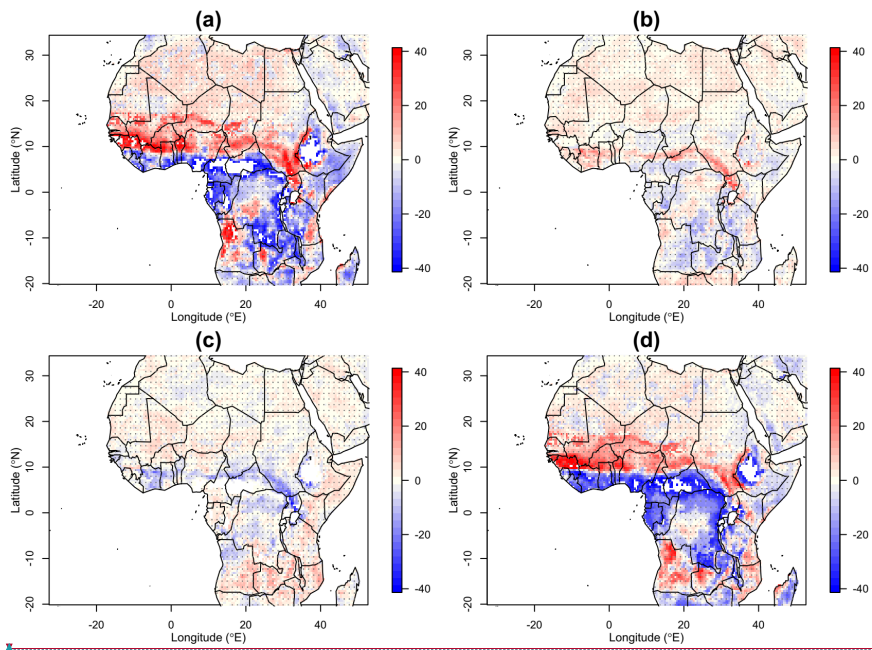


**Figure 4.** Difference of drought frequencies between the DV and the SV ensembles (a) for the historical period (1981-2000) and (d) for the future period (2081-2100). Differences between the future and historical periods (future-historical) for (b) SV ensembles and (c) DV ensembles. Drought frequency is defined for events with an SPEI less than -1. Dotted region shows areas passing the two-tailed confidence level with  $\alpha=0.01$ .

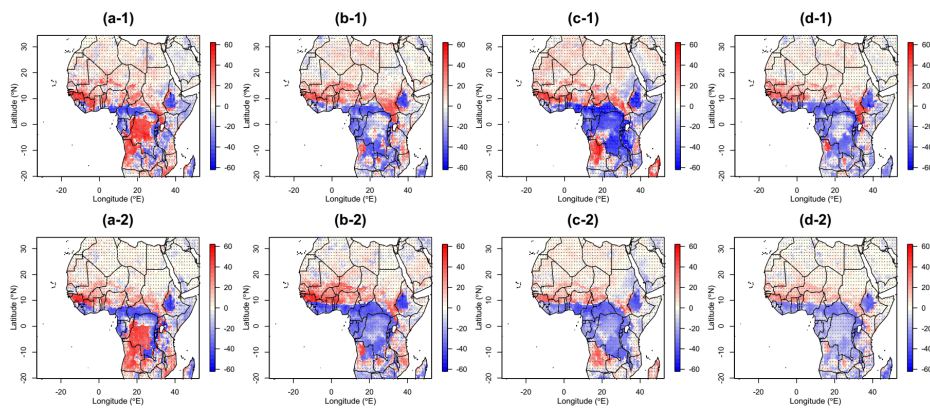
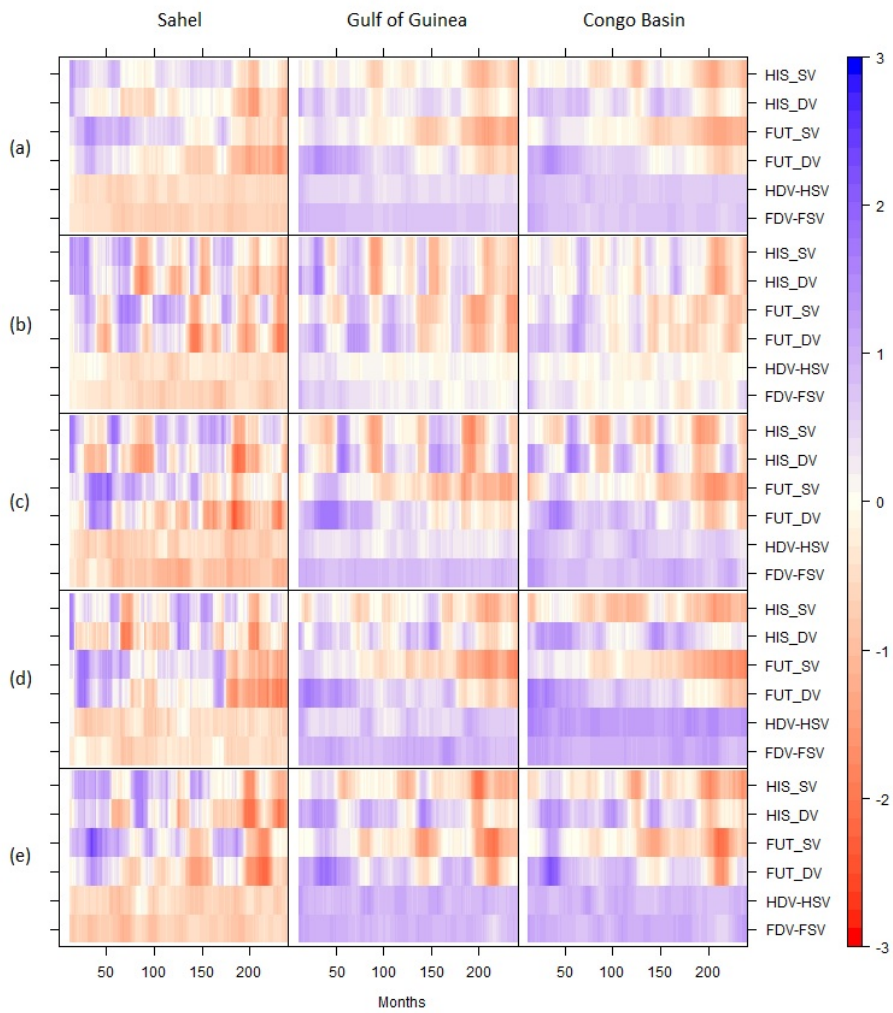


**Figure 5.** Difference of drought frequencies between the DV and the SV ensembles (1) for the historical period (1981-2000) and (2) for the future period (2081-2100) from the ensemble members with different LBCs of (a) CCSM, (b) GFDL, (c) MIROC and (d) MPI-ESM. Drought frequency is defined for events with an SPEI less than -1. Dotted region shows areas passing the two-tailed confidence level with  $\alpha=0.01$ .

**Deleted:**

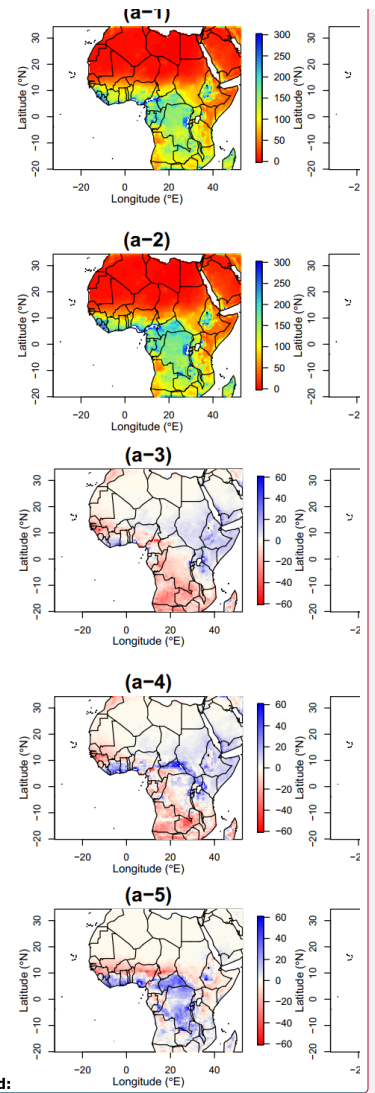
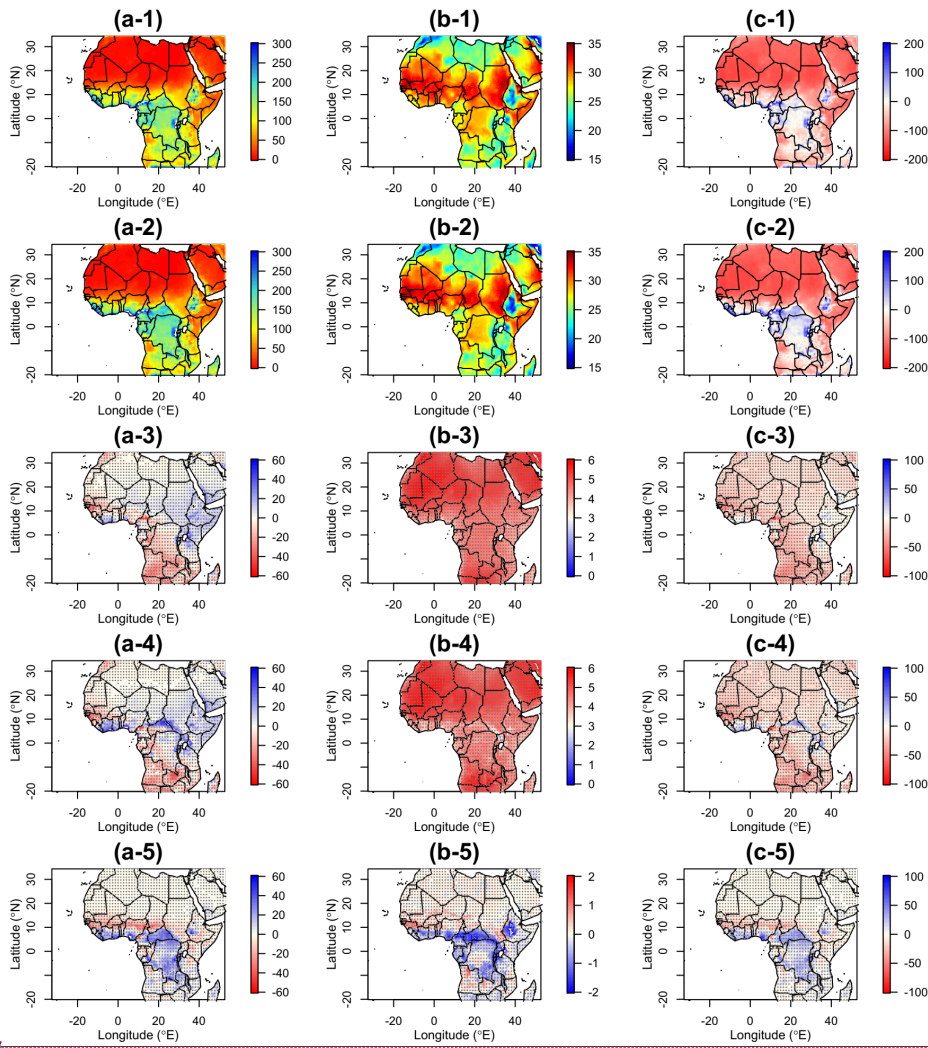
**Formatted:** Font color: Text 1

**Formatted:** Font color: Text 1





68 **Figure 6.** Monthly SPEI averaged for three regions of the Sahel, the Gulf of Guinea, and the Congo Basin in (a) ensembles and the individual  
69 member with different LBCs of (b) CCSM, (b) GFDL, (c) MIROC and (d) MPI-ESM. HSV and HDV (FSV and FDV) represent the historical  
70 (future) simulation without and with dynamic vegetation, respectively. HDV-HSV (FDV-FSV) depict the difference between HDV and HSV  
71 (FDV and FSV).



Deleted:  
Formatted: Font color: Text 1

.75 **Figure 7.** Averages of simulated (a) precipitation (mm/month) and (b) temperature (°C), and (c) derived precipitation surplus/deficit  
.76 (mm/month) from 1) SV ensembles and 2) DV ensembles for the future period of 2081–2100. Their difference between future and historical  
.77 periods (future-historical) for 3) SV ensembles and 4) DV ensembles are shown. The difference between DV and SV ensembles reflect the  
| .78 future period. Doted region shows areas passing the two-tailed confidence level with  $\alpha=0.01$ .

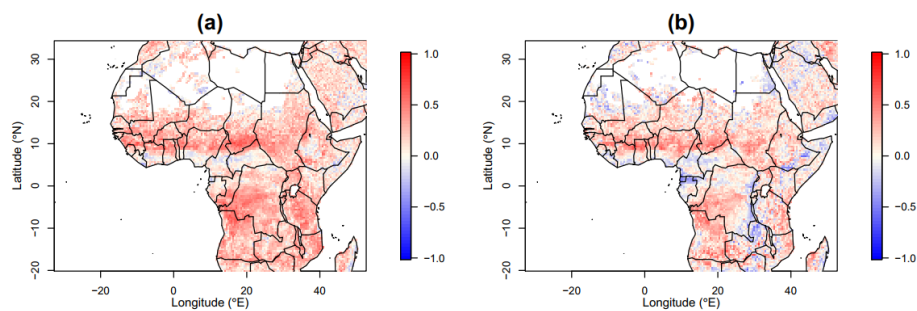


**Figure 8.** Spearman's rank correlation coefficient between annual minimum LAI and annual maximum SPEI from the DV ensembles for (a) the historical (1981-2000) and (b) future (2081-2100) periods.

Boundary conditions from different GCMs	CCSM	Community Earth System Model
	GFDL	Geophysical Fluid Dynamics Laboratory
	MIROC	Model for Interdisciplinary Research on Climate-Earth System Model
	MPI-ESM	Max Planck Institute Earth System Model
Vegetation dynamics	DV	Dynamic Vegetation
	SV	Static Vegetation
Periods	Historical	1981–2000
	Future	2081–2100

Deleted: ... [2]